Structural and magnetic phases of ultrathin Fe wedges and films grown on diamond (100)

Dongqi Li, D. J. Keavney,* J. Pearson, and S. D. Bader
Materials Science Division, Argonne National Laboratory, Argonne, Illinois 60439

J. Pege and W. Keune
Laboratorium für Angewandte Physik, Gerhard-Mercator-Universität, D-47048 Duisburg, Germany
(Received 20 October 1997)

Fe wedges (0–20 Å) and films have been grown epitaxially onto diamond C(100) substrates, and their metastable structural and magnetic phases were studied by means of reflection high-energy electron diffraction (RHEED), the surface magneto-optic Kerr effect (SMOKE), and *in situ* Mössbauer spectroscopy. Both the substrate and films $\leqslant 5$ ML thick, that were grown at room temperature and subsequently annealed, show 1×1 streaks in the RHEED patterns, indicating a flat, well-ordered fcc structure. Films >5 ML thick exhibit a three-dimensional bcc RHEED pattern. No magnetic signal was observed in either longitudinal or polar SMOKE measurements that were taken between 120 and 300 K for Fe thickness <5 ML. For >5.5-ML Fe, the films are ferromagnetic with in-plane easy axis, and the saturation magnetization (at 130 K) increases linearly with Fe thickness. *In situ* Mössbauer spectra for a 4-ML-thick ^{57}Fe film exhibit a spectral line typical of paramagnetic fcc Fe at 300 and 70 K. This line broadens considerably at 40 and 35 K due to magnetic hyperfine interaction, indicating a low-moment antiferromagnet. These results indicate that 5 ML is the fcc-bcc phase boundary that separates low-moment antiferromagnetic from ferromagnetic ground states, respectively. [S0163-1829(98)05216-3]

I. INTRODUCTION

Face-centered-cubic (fcc) Fe (γ-Fe) is predicted to have ferromagnetic and antiferromagnetic phases depending on atomic volume.[1] In nature, the room-temperature (RT) phase of Fe is bcc and ferromagnetic, while the fcc phase occurs between 1184 and 1664 K. The fcc Fe lattice constant (a) extrapolated down to RT is 3.59 Å. Epitaxy of Fe on different substrates permits fcc-like phase stabilization with expanded or contracted in-plane lattice constants. Fe on Cu(100) ($a=3.61$ Å) is a well-studied example, where the interplay between structural and magnetic instabilities is clearly manifested with several face-centered structural and magnetic phases under different growth conditions.[2–6] RT-grown films 2–5 ML thick are ferromagnetic, with a face-centered-tetragonal (fct) structure, while those 6–11 ML thick have an enhanced ferromagnetic surface and an antiferromagnetic (AFM) interior, composed of alternating ferromagnetic layers.[2] The complex multiplicity of phases were recently described theoretically as arising from frustrated exchange interactions.[7] fcc Fe on fcc Co(100),[8,9] Ni(100),[8] Cu-Au alloys,[5,10] and $Ni_{81}Fe_{19}$(100) (Ref. 11) have also been investigated. All these cases represent expansion of the fcc Fe lattice, and yield similar structural and magnetic phases as Fe/Cu(100). Diamond (100), on the other hand, has a lattice constant of 3.57 Å, and thus provides an in-plane *contraction* for metastable fcc Fe. fcc Fe has been grown onto synthetic C(100),[12,13] though the magnetic characterization is inconclusive. In this work, we investigate wedge-shaped Fe films of 0–20 Å on diamond (100) by means of reflection high-energy electron diffraction (RHEED), low-energy electron diffraction (LEED), and the surface magneto-optical Kerr effect (SMOKE) in order to identify the structural and magnetic phases systematically. In addition, we have employed Mössbauer spectroscopy on a 4-ML-thick ^{57}Fe film to provide local information about magnetism and structure via the hyperfine parameters. We observed that Fe grows onto diamond (100) as two-dimensional (2D) epitaxial, fcc films for the first 5 ML, and is paramagnetic at RT and low-spin AFM at low temperature. Fe thicknesses >5 ML are rough, bcc, and ferromagnetic, as expected for the bcc phase. These results are in contrast with those of the expanded cases of epitaxial fcc Fe films.[2–6,8–11]

II. EXPERIMENT

The work at Argonne was carried out in a UHV chamber ($<1\times10^{-10}$ Torr) equipped with SMOKE, low-energy electron diffraction (LEED), RHEED, Auger spectroscopy, and joule-heated evaporators. Synthetic diamond substrates of 4×4 mm^2 were used for systematic structural and SMOKE measurements. The diamond C(100) substrates were prepared by etching in $HCl:HNO_3$ solution and boiling in $H_2O:H_2O_2:NH_4OH$ solution, followed by ultrasonic cleaning in distilled water. The substrates were then transferred into the UHV chamber with a load-lock system, and cleaned by heating to 650 °C. The Fe films were grown at RT under a typical pressure of 1×10^{-9} Torr, and subsequently annealed to 400 °C after each ~5-Å Fe dosage. Previous work has shown that deposition at RT followed by a 600 °C anneal results in the carbon-stabilized fcc Fe phase as in stainless steel.[13] Our RT deposition results in no structural ordering above 2.5 ML, as observed by RHEED. We anneal at a relatively low temperature to minimize interdiffusion at the interface, yet ensuring the formation of fcc Fe films. The nominal Fe thickness was determined with a quartz-crystal thickness monitor within an accuracy of ~20%, assuming a fcc structure. A typical deposition rate was ~0.2 Å/min.

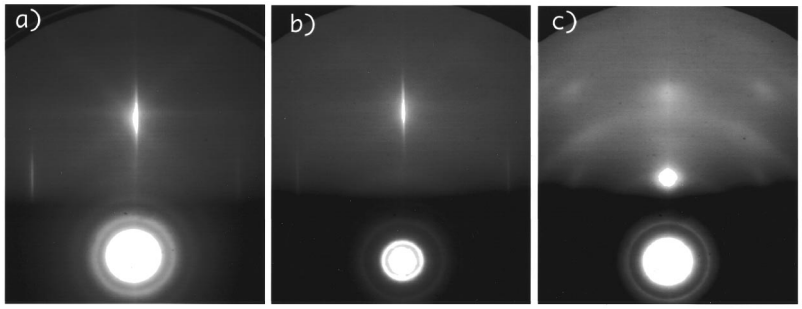

FIG. 1. Typical RHEED pictures taken at electron energy of 9 kV with a CCD camera. (a) Clean C(100) substrate. (b) 4.0-ML Fe/C(100). (c) 7.8-ML Fe/C(100).

Wedge-shaped samples have a typical slope of 1–2 Å/mm. The cleanliness and surface structure of the substrates and the films were confirmed with Auger, RHEED, and LEED. Several substrates were used during the experiment, each repeatedly etched outside the UHV chamber after Fe deposition and reused. Magnetic properties were measured *in situ* via SMOKE utilizing a focused He-Ne laser beam ($\sim$0.2 mm in diameter) scanned along an Fe wedge to obtain hysteresis loops from the Kerr ellipticity. Both longitudinal and polar measurements were performed between 120 and 300 K.

Mössbauer measurements at Duisburg utilized a 4.0 $\pm$0.8-ML-thick film of 95.5% isotopically enriched ^{57}Fe grown at RT in a UHV chamber (base pressure $<8\times10^{-11}$ Torr) at a rate of 0.48 Å/min under a background pressure of 5×10^{-10} Tor. The substrate was a natural diamond C(100) of 6×6-mm^2 area. Chemical etching was as described above. After transferring the substrate into the UHV chamber, it was cleaned by annealing at 900 °C for 10 min. The nominal Fe thickness was measured by a quartz-crystal thickness monitor calibrated previously by RHEED-intensity oscillations from fcc-Fe/Cu(100). The cleanliness and surface structure of the films were determined by Auger and RHEED. The ^{57}Fe conversion-electron Mössbauer spectra (CEMS) were obtained *in situ* utilizing a channeltron detector. The γ radiation from a $\sim$100-m Ci ^{57}Co(Rh) Mössbauer source was incident normal to the film plane. All isomer-shift (δ) values are given relative to bulk α-Fe at RT.

III. RESULTS AND DISCUSSIONS

Figure 1 shows typical RHEED patterns of a synthetic C(100) substrate, and Fe films of 4.0 and 7.8 ML. Both the substrate and films <5 ML thick show sharp 1×1 patterns with similar spacings, indicating a well-ordered fcc structure. The substrate and film surfaces are reasonably flat, as indicated by the sharp streaks in the RHEED pattern. Films >5 ML thick exhibit a 3D spotty RHEED pattern, as shown in Fig. 1(c). Some ring-shaped features are also evident, suggesting the coexistence of a polycrystalline phase. RT deposition only results in the fading of the 1×1 diamond (100) RHEED pattern, which disappears above 2.5 ML. This suggests that, at RT, Fe cannot form an ordered fcc film. The lattice spacings of the annealed films can be measured from the spacing on the RHEED pattern compared with that of the C(100) reference. The Fe films first grow pseudomorphically with the in-plane lattice spacing the same as that of diamond (100) (1.795 Å). The 3D phase has a relaxed lattice spacing; the in-plane separation of atom rows *perpendicular to the diffraction plane* is 2.04 ± 0.02 Å. This coincides with the row distance of 2.03 Å for bcc Fe along the [110] direction. Such an orientation is consistent with a transformation to the bcc structure, with its [111] direction matching the fcc [110] as occurs in the fcc-to-bcc transformation of Fe/Cu(100).[14] Assuming this orientational relationship to be the case, the atomic row distance should be reported relative to [110] rather than perpendicular to the diffraction plane. This small correction yields a spacing of 2.01 ± 0.02 Å along the [110] direction, again in excellent agreement with expectation. Therefore, films thicker than 5 ML are essentially of bcc structure. It is noted that the fcc structure is retained for a thicker film when the source and/or the substrate are dirty. This is, however, normally accompanied by a $c(2\times2)$ reconstruction. This is attributed to surfactant-mediated growth as occurs in Fe/Cu(100), where an fcc layer-by-layer growth can persist up to 40 ML or more in comparison to 10–11 ML for clean Fe/Cu(100).[15,16]

In addition to the spacing, the *width* of the streaks and/or spots also changes drastically between Figs. 1(a) and 1(b) and Fig. 1(c). The broadening of the streak width indicates a decrease in the average terrace size, i.e., a rougher surface. This accompanies the transformation into the 3D bcc phase. In general, the width of a streak (w) includes an instrumental broadening, but, ignoring this, we can estimate the lower limit of the terrace sizes as $2\pi/w\sim450$ Å for the 4-ML fcc phase [Fig. 1(b)], and ~150 Å for the 7.8-ML bcc phase [Fig. 1(c)].

Plotted in Fig. 2 are the row spacing in real space and the lower limit of terrace size $2\pi/w$ from the RHEED patterns along a wedge as a function of the nominal Fe thickness, assuming an fcc structure and 1 ML$=1.8$ Å. There is an abrupt change in both the row spacing and the terrace size at ~5 ML. This indicates a structural phase transition from a fcc (100) film to a bcc (110) texturing. This structural phase transition may possess quantitative differences on different substrate crystals or on the same crystal after each etching. For example, for some wedges, the transition is more gradual than the one indicated in Fig. 2. Nevertheless, the transition always occurs at ~5 ML. These minor differences may be caused by different defect densities on the substrates.

Figure 3 shows typical LEED patterns for 3.2- and 7.8-ML-thick Fe along the same wedge as in Figs. 1 and 2. Both show the same fcc 1×1 pattern as that of the diamond substrates, though the one for 7.8 ML has a slightly higher back-

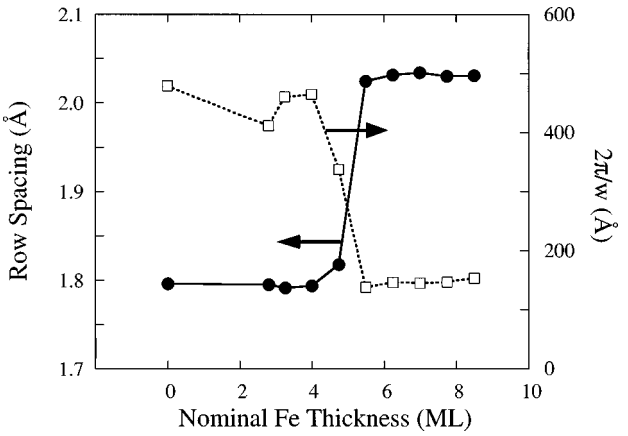

FIG. 2. The row spacing and the lower limit of average terrace size $2\pi/W$ in real space from the RHEED patterns along an Fe wedge on diamond (100), where W is the width of the streaks in the RHEED patterns. A structural phase transition is apparent at ~ 5 ML.

ground. No bcc phase can be identified. This apparent conflict with the RHEED results may be due to the exposed fcc C(100) substrate or to residual fcc Fe film after the Fe balls up to form tiny 3D bcc grains. This is consistent with the fact that the bcc phase is very rough, based on our RHEED results. RHEED, with a glancing incidence, is most sensitive to the top surface of a film, while LEED, with a normal-incidence electron beam, is sensitive not only to the film, but also to any exposed substrate. Our Auger measurements reveal a C signal even for the thickest films, which may come from exposed substrate or C interdiffusion.

Figure 4 shows typical SMOKE longitudinal hysteresis loops along an Fe wedge. No magnetic signal was observed in either longitudinal or polar measurements for Fe thickness <5 ML. For >5.5-ML Fe, the films are ferromagnetic, with in-plane easy axis. Both the saturation magnetization (M_s) at 130 K and the Curie temperature (T_C) of the film increase linearly with Fe thickness, as seen in Fig. 5. Linear fits of the M_s and T_C indicate that they extrapolate to zero at around 5 ML, instead of 0 ML, which further quantifies the onset of ferromagnetic ordering. T_C increases from 120 to 300 K within 1 ML of the onset of ferromagnetism along the wedge. This onset at ~ 5 ML coincides with the onset of the structural phase transition from fcc to bcc. These results indicate that the metastable, epitaxial fcc Fe films (<5 ML)

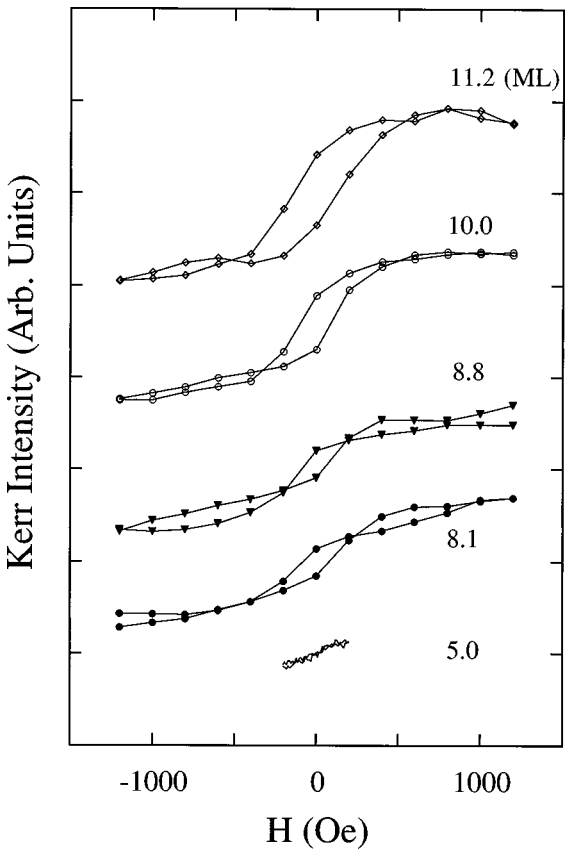

FIG. 4. Longitudinal Kerr hysteresis loops of Fe/C(100) taken at 130 K. No magnetic signal, polar or longitudinal, was detected for films <5 ML.

are not ferromagnetic above 120 K. Only the ordinary bcc films are ferromagnetic as expected.

Typical CEM spectra obtained at different temperatures from the annealed 4.0-ML-thick ^{57}Fe film on natural C(100) are shown in Fig. 6. The RHEED pattern of this film (not shown) is similar to that shown in Fig. 1(b), except that the RHEED streaks are considerably broadened. This indicates that the 4-ML ^{57}Fe film is fcc, but is much rougher than the one in Fig. 1(b).

Evidence for the fcc structure and paramagnetism of the 4-ML ^{57}Fe film are obtained from the CEM spectrum at RT (Fig. 6, top). No lines of ferromagnetic α-Fe are observed. Data analysis by a least-squares computer fit[17] with Lorent-

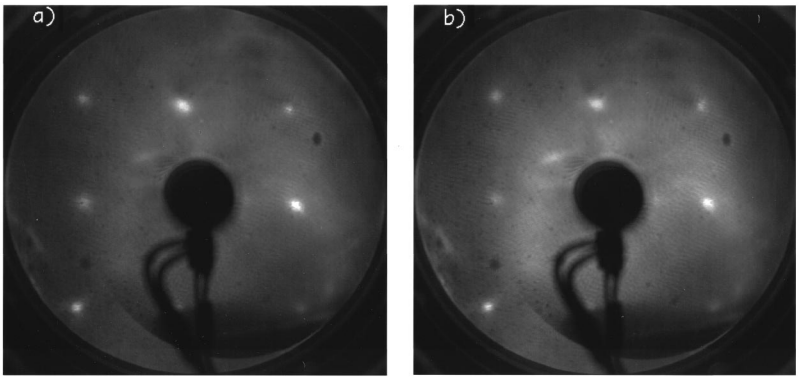

FIG. 3. Typical LEED patterns of Fe/C(100) taken at an electron energy of 145 eV. (a) 3.2 ML. (b) 7.8 ML.

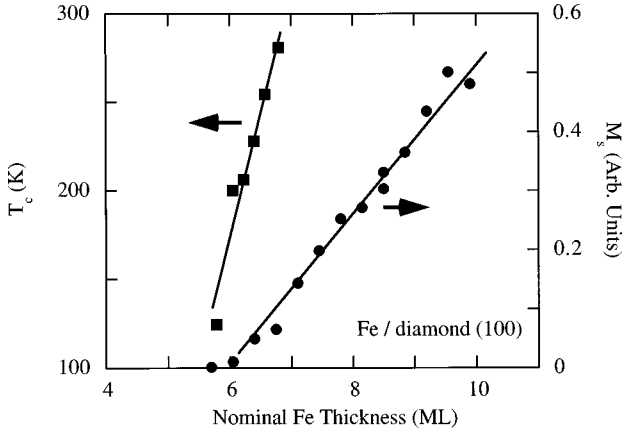

FIG. 5. The saturation magnetization M_s at $T=130$ K, and the Curie temperature T_C along an Fe wedge on C(100).

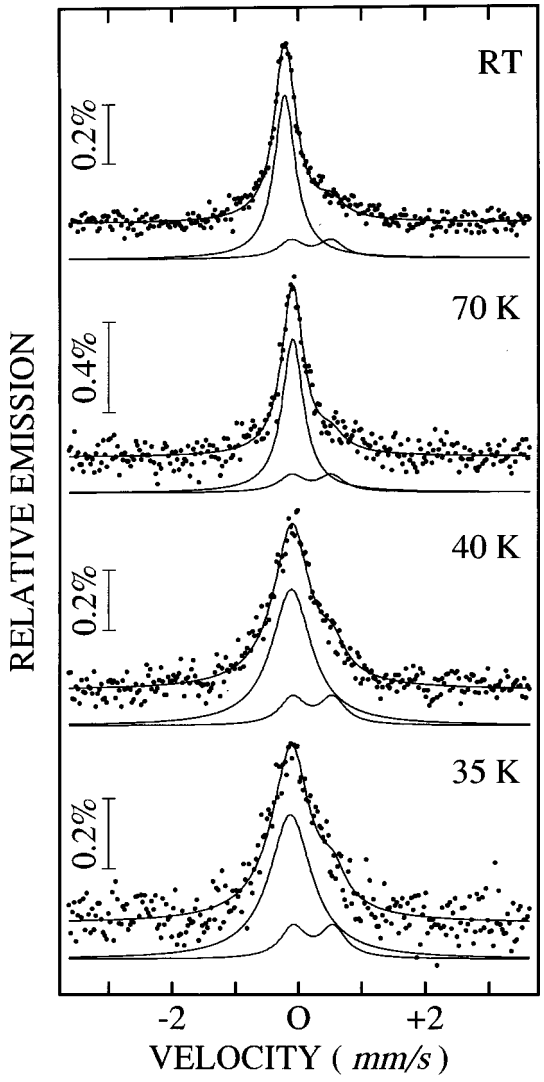

FIG. 6. Mössbauer spectra of annealed 4.0-ML Fe/C(100) measured at RT, 70, 40, and 35 K (from top to bottom, respectively). The linewidths of the fitted central line are 0.40 ± 0.01, 0.41 ± 0.02, 0.76 ± 0.03, and 0.81 ± 0.05 mm/s, respectively.

zian lines yield a dominant (rather narrow) central line (of 80% in relative spectral area) and a less-intense (symmetric) quadrupole-split doublet (satellite spectrum, of 20% in relative spectral area). The strong central line exhibits an isomer shift δ of -0.101 ± 0.009 mm/s at 300 K. This negative value is very close to that of paramagnetic fcc γ-Fe precipitates in a Cu matrix at 300 K ($\delta=-0.088\pm0.003$ mm/s),[18–21] and is close to isomer-shift values of paramagnetic fcc Fe/Cu(100) multilayers[22,23] and films[24,4] at RT ($\delta=-0.08\pm0.01$ mm/s). Therefore, we assign the central single line in Fig. 6 to paramagnetic fcc Fe on C(100). The measured full width at half maximum Γ of this single line is 0.40 ± 0.01 mm/s at RT, and remains unchanged at 70 K ($\Gamma=0.41\pm0.02$ mm/s). This indicates that fcc Fe on C(100) is still paramagnetic at 70 K.

The dominant fcc Fe line is found to broaden considerably at low temperatures (Fig. 6). For example, Γ of 0.76 ± 0.03 and 0.81 ± 0.05 mm/s is obtained at 40 and 35 K, respectively. This observation is analogous to the case of AFM fcc Δ-Fe precipitates in Cu below their Néel temperature of 67 K, where a reduction in temperature leads to increasing line broadening due to an increasing degree of AFM ordering.[18–21] The AFM state is indicated by a line broadening only, since the magnetic hyperfine-field saturation value ($\sim$2.4 T for large precipitates) is of the order of the natural linewidth, and thus the full ^{57}Fe six-line Zeeman pattern of fcc Fe cannot be resolved. This is a consequence of the low Fe atomic magnetic moment ($\sim0.7\mu_B$) of these AFM γ-Fe precipitates.[25,26]

Similar drastic line broadening at low temperatures has been reported for fcc-Fe/Cu(100) multilayers[22,23] ($\Gamma=0.8$ mm/s at 4.2 K, equivalent to a hyperfine field $B_{\rm hf}\approx1.6$ T) and fcc Fe/Cu(100) films[24,4] ($\Gamma=0.5-0.6$ mm/s at 29–35 K, equivalent to $B_{\rm hf}=1.1-1.3$ T). Moreover, AFM ordering at 4.2 K in fcc Fe/Cu(100) multilayers has been proven by Mössbauer spectroscopy in an external magnetic field.[22] The average magnetic hyperfine field estimated from the linewidth of our film is about 1.3–1.5 T at 40–35 K, thus being in agreement with typical $B_{\rm hf}$ values for the AFM fcc Fe/Cu(100) system and for AFM γ-Fe precipitates in Cu. Therefore, we conclude that annealed 4-ML-thick fcc Fe on C(100) is in a low-moment AFM state at low temperature. This identification clearly rules out the possibility of having superparamagnetism below 5 ML.

It is interesting to note that the width of the paramagnetic fcc Fe/C(100) line at RT ($\Gamma=0.40\pm0.01$ mm/s) is slightly larger than the corresponding value of 0.30 ± 0.01 mm/s in fcc Fe/Cu(100),[22,23,24,4] and is remarkably larger than the linewidth observed with our spectrometer on a standard α-Fe calibration foil (0.24–0.26 mm/s). The excess linewidth in the case of fcc Fe/C(100) might be caused by interstitial C impurities. It is well known that in C-containing paramagnetic (bulk) fcc steel (austenite), the electron distribution at nearest-neighbor Fe atoms surrounding an interstitial C impurity is perturbed, giving rise to a quadrupole splitting $\Delta E_Q=e^2qQ/2$ of about 0.625–0.643 mm/s, and a δ of about $-0.06--0.002$ mm/s at RT.[27–29] Fe atoms more distant from a C impurity show the characteristic fcc-Fe single line of paramagnetic austenite with a δ of $-0.05--0.1$ mm/s at RT.[27,28] The intensity (area) ratio of the single line to the quadrupole doublet depends on the C concentration in the

austenite. This poses a question about the origin of the quadrupole-split doublet (satellite spectrum) included in the least-squares fitting of the data in Fig. 6. While the ΔE_Q value of 0.63 mm/s of this doublet agrees well with that of Fe atoms with one nearest-neighbor C atom in austenite, the isomer shift of this doublet in Fig. 6 is $+0.28\pm0.05$ mm/s at RT, which is far from the corresponding δ value in austenite. Therefore, one has to look for another explanation of the doublet in Fig. 6. As a possibility, it could originate from the paramagnetic fcc Fe/diamond interface. A quadrupole doublet with similar splitting ($\Delta E_Q = 0.60 \pm 0.08$ mm/s), though with a different isomer shift of -0.015 ± 0.005 mm/s, has been observed at 300 K for probe-layer ^{57}Fe atoms artificially located at the paramagnetic fcc Fe/Cu(100) interface.[4] Similar work on the fcc Fe/C(100) interface is in progress to clarify the origin of the doublet. Due to the much larger intensity of the fcc Fe single line in Fig. 6, our results for fcc Fe are essentially independent of the detailed shape of the weak satellite doublet.

The formation of a low-spin AFM phase for thin fcc Fe is in contrast to the Fe/Cu(100) case. For Fe/Cu(100), a high-spin ferromagnetic phase exists for both RT- and low-temperature-grown films, at least when the Fe thickness is <5 ML. This high-spin Fe/Cu phase has a metastable fct structure with reconstructions.[30] There are several possible causes for this difference, such as lattice contraction instead of expansion, carbon interdiffusion, etc. It is interesting to mention that low-temperature-grown fcc Fe/Cu(100) films, which are in a ferromagnetic high-moment state before annealing,[2] are highly metastable and can be transformed to the more stable AFM low-moment fcc Fe phase by annealing at $\sim$570 K ($\sim$300 °C) and cooling to RT.[4] We postulate that the AFM fcc Fe films on C(100) might behave in a similar fashion after annealing.

IV. CONCLUSIONS

We have studied the structural and magnetic phases of annealed Fe films on diamond (100). Films of <5 ML exhibit 2D epitaxial growth and form a fcc phase. From SMOKE, such a phase is found not to be ferromagnetic above 120 K, the lowest temperature explored. Films thicker than 5 ML transform into a 3D bcc phase, which is the normal ferromagnetic phase. A Mössbauer spectral line typical for paramagnetic fcc ^{57}Fe was observed for 4-ML Fe at and above 70 K, while at and below 40 K the film is in a low-moment antiferromagnetic state.

ACKNOWLEDGMENTS

We thank Dr. D. Pappas for valuable information and discussions, and Dr. S. Jiang and U. von Hörsten for technical assistance. One of us (W.K.) is grateful to the Volkswagen Stiftung for supporting his stay at Argonne. The work at Argonne was supported by the U.S. Department of Energy, BES-MS, under Contract No. W-31-109-ENG-38, and at Duisburg by the Deutsche Forschungsgemeinschaft (SFB 166).

*Present address: Department of Physics, University of Arizona, Tucson, AZ 85721.

[1] C. S. Wang, B. M. Klein, and H. Krakauer, Phys. Rev. Lett. **54**, 1852 (1985); V. L. Moruzzi, P. M. Marcus, K. Schwarz, and P. Mohn, Phys. Rev. B **34**, 1784 (1986); F. J. Pinski, J. Staunton, D. D. Johnson, and G. M. Stocks, Phys. Rev. Lett. **56**, 2096 (1986).

[2] J. Thomassen, F. May, B. Feldmann, M. Wuttig, and H. Ibach, Phys. Rev. Lett. **69**, 3831 (1992).

[3] Dongqi Li, M. Freitag, J. Pearson, Z. Q. Qiu, and S. D. Bader, Phys. Rev. Lett. **72**, 3112 (1994), and references therein.

[4] W. Keune, A. Schatz, R. D. Ellerbrock, A. Fuest, Katrin Wilmers, and R. A. Brand, J. Appl. Phys. **79**, 4265 (1996).

[5] D. J. Keavney, D. F. Storm, J. W. Freeland, I. L. Grigorov, and J. C. Walker, Phys. Rev. Lett. **74**, 4531 (1995).

[6] M. Zharnikov, A. Dittschar, W. Kuch, C. M. Schneider, and J. Kirschner, Phys. Rev. Lett. **76**, 4620 (1996).

[7] D. Spisak and J. Hafner, Phys. Rev. B **56**, 2646 (1997).

[8] W. L. O'Brien and B. P. Tonner, Phys. Rev. B **52**, 15 332 (1995).

[9] Ernesto J. Escorcia-Aparicio, R. K. Kawakami, and Z. Q. Qiu, Phys. Rev. B **54**, 4155 (1996); Ernesto J. Escorcia-Aparicio, H. J. Choi, R. K. Kawakami, and Z. Q. Qiu, J. Appl. Phys. **81**, 4714 (1997).

[10] D. Tillmann and E. Kisker, Solid State Commun. **100**, 415 (1996).

[11] W. Kuch and S. S. P. Parkin, Europhys. Lett. **37**, 465 (1997).

[12] D. P. Pappas, J. W. Glesener, V. G. Harris, Y. U. Idzerda, J. J. Krebs, and G. A. Prinz, Appl. Phys. Lett. **64**, 28 (1994).

[13] R. S. Swineford, D. P. Pappas, and V. G. Harris, Phys. Rev. B **52**, 7890 (1995).

[14] K. Kalki, D. D. Chambliss, K. E. Johnson, R. J. Wilson, and S. Chiang, Phys. Rev. B **48**, 18 344 (1993).

[15] Dongqi Li, M. Freitag, J. Pearson, Z. Q. Qiu, and S. D. Bader, J. Appl. Phys. **76**, 6425 (1994).

[16] A. Kirilyuk, J. Giegiel, J. Shen, M. Straub, and J. Kirschner, Phys. Rev. B **54**, 1050 (1996).

[17] For least-squares fitting of the data, the computer program by R. A. Brand, provided by WISSEL GmbH., D-82319 Starnberg, Germany, has been used.

[18] U. Gonser, C. J. Meechan, A. H. Muir, and H. Wiedersich, J. Appl. Phys. **34**, 2373 (1973).

[19] S. J. Campbell and P. E. Clark, J. Phys. F **4**, 1073 (1974).

[20] D. L. Williamson, W. Keune, and U. Gonser, *Proceedings of the International Conference on Magnetism* (Nauka, Moscow, 1974), Vol. 1, p. 246.

[21] T. Ezawa, W. A. A. Macedo, U. Glos, W. Keune, K. P. Schletz, and U. Kirschbaum, Physica B **161**, 281 (1989).

[22] W. Keune, R. Halbauer, U. Gonser, J. Lauer, and D. L. Williamson, J. Appl. Phys. **48**, 2976 (1977).

[23] R. Halbauer and U. Gonser, J. Magn. Magn. Mater. **35**, 55 (1983).

[24] W. A. A. Macedo and W. Keune, Phys. Rev. Lett. **61**, 475 (1988).

[25] S. C. Abrahams, L. Guttmann, and J. S. Kasper, Phys. Rev. **127**, 2052 (1962).

[26] G. J. Johanson, M. B. McGirr, and D. A. Wheeler, Phys. Rev. B **1**, 3208 (1970).

[27] P. M. Gielen and R. Kaplow, Acta Metall. **15**, 49 (1967).

[28] J. M. Genin and P. A. Flinn, Phys. Lett. **22**, 392 (1966).

[29] S. J. Lewis and P. A. Flinn, Phys. Status Solidi **26**, K51 (1968).

[30] S. Müller, P. Bayer, C. Reischl, K. Heinz, B. Feldmann, H. Zillgen, and M. Wuttig, Phys. Rev. Lett. **74**, 765 (1995).